J. King Saud Univ., Vol. 20, *Eng. Sci.* (1), pp. 47-60, Riyadh (2008/1429H.)

Practical Well Test Analysis of a Hydraulically Fractured Low Permeability Gas Reservoir: A Case History

Hazim N. Dmour

Department of Petroleum and Natural Gas Engineering, College of Engineering, King Saud University, P.O. Box 800, Riyadh 11421, Saudi Arabia

(Received 21 November 2006; accepted for publication 25 February 2007)

Keywords: Hydraulic fracturing, Low permeability gas reservoir, Gas well performance, Non-Darcy effect, Finite conductivity fracture, Modified isochronal test.

Abstract. The primary objective of hydraulic fracturing is to create a propped fracture with sufficient conductivity and length to amplify or at least optimize well performance of low permeability tight gas reservoir. The oil industry has suggested that hydraulically fractured tight gas wells performance is hindered significantly by non-Darcy flow effect.

This work will present an investigation of non-Darcy flow effect to hydraulically fractured gas wells performance and provide the development, validation, and application of actual well test analysis for wells with a finite conductivity vertical fracture.

Also, this work presents the results obtained in the study of actual post frac modified isochronal test data of gas wells intersected by a finite conductivity vertical fracture in a tight low permeability gas reservoir. In addition, the estimation of reservoir properties and fracture properties were carried out to construct a simple analytical model, which used for rate prediction.

The effect of non-Darcy flow in fractures is clearly seen in the tests data and will lead to limiting production especially on higher chokes (after one inch). Therefore, non-Darcy effects should be considered in design of hydraulic fracture treatments, otherwise the design might be far from optimal

Introduction

Hydraulic fracturing is used extensively for improving the productivity of tight, low permeability gas reservoir, and much work has been performed to develop models for analyzing vertically fractured gas wells. The ultimate performance of fractured wells is severely diminished by the effects of non–Darcy flow inside the fracture. Several authors (Horne, 1995; Cinco-Ley *et al.*, 1985; Fetkovich, 1980) agree that the most important variable affecting proppant pack permeability is the non-Darcy flow. (Lee and Holditch, 1981) mention that high pressure drop due to high velocities that might be due to both turbulence and inertial resistance. Also, they pointed out that effected of non-Darcy flow on gas well productivity index is a function of proppant type and not to consider it might result in a wrong analysis of well test interpretation.

Regarding pressure transient analysis on both hydraulically and naturally fractured reservoir, a review of the literature shows that it was initially discussed by (Pollard, 1959). He was interested on the determination of fracture volume from pressure build-up tests. In deep reservoirs, the induced fractures are generally vertical and tend to follow a single plane of weakness. The presence of vertical fracture at the wellbore complicates the transient flow behavior of a low permeability gas well. The flow is further complicated when turbulence occurs near the wellbore.

(Russell and Truit, 1964) published transient drawdown solutions for vertically fractured liquid wells. They developed methods of drawdown and build-up testing utilizing these solutions, which were based in numerical simulation. (Clark, 1968) applied the basic Russell Truitt solutions to analyze fractured water injection wells by falloff test.

The works of (Mattar *et al.*, 2006) collects and summarizes several important developments in pressure transient analysis and emphasizes how to

practically apply them to the design and analysis of fractured well tests.

(Cringarten *et al.*, 1972) reviewed the theory on transient pressure analysis for both hydraulically and naturally fractured reservoirs. Later, (De Swaan, 1976) presented analytical unsteady sate solution for a well producing at constant flow rate in naturally fractured reservoirs; he introduced new diffusivity definitions useful for reservoir characterization.

(Crawford *et al.*, 1976) have presented some of the best field examples of pressure transient tests on both hydraulically and naturally fractured reservoirs. In fractured wells, the study (Partikno, 2003) reported that tests on hydraulic fractured wells often matched the early fractured type curves but yield apparent fracture length of 10 ft when the design lengths where more than 1000 ft. An early study by (Holditch *et al.*, 1976) attributed this to high velocity flow in a fracture. But, the work by (Ramey, 1965) indicated that finite–fracture permeability-width was a more likely cause of the problem. They used a finite–element solution. (Prats, 1961) provided the key to this problem in classic study on steady-state flow. (Cinco-Ley *et al.*, 1986) presented a truly classic semi-analytical, real domain solution for a well with a finite conductivity vertical fracture in an infinite acting reservoir. This semi analytical solution is tedious, but accurate.

All works presented above address very well the effects of fracture design changes on the well performance. An analytical model obtained from different sources has been used in this work without considering the impact of the equations selection on the final results. In this paper, a systematic evaluation of Modified Isochronal Test of hydraulically fractured two gas wells was performed to examine the effect and magnitude of non-Darcy flow on pseudo-steady state productivity index (of stimulated gas well). In addition, this paper shows an application of this technique to the hydraulically fractured low permeability tight gas reservoir and demonstrates how build-up and drawdown data dominated totally by bilinear flow, which can be rigorously evaluated with this concept, and by computer model.

Physical Model-identification of Flow Regime

The finite Conductivity Fracture Model simulates a well that is intercepted by a finite conductivity vertical fracture (Fig. 1). The well is contained in a circular shaped reservoir with an infinite-acting or no-flow outer boundary. At early times, this model utilizes the concept of (Lee *et al.*, 1986) of tri-linear flow to represent a finite conductivity fracture (Fig. 2). Three linear-flow zones that dominate the pressure behavior are:

- Fracture flow in the X-direction.
- Formation flow in Y-direction.
- Formation flow in X-direction.

Fracture diffusivity has been assumed constant at 1 E6, as suggested by (Cinco-Ley *et al.*, 1979). The tri-linear fracture flow results merge into the solution for infinite-acting radial flow in the middle times. Thus, the tri-linear flow solution is truncated as soon as the flow becomes pseudo-radial. Occasionally, the merging of these two solutions is not smooth, and the derivative exhibits spikes. These are localized aberrations and can be ignored as they do not affect the rest of the results. Ultimately, at late times, the model uses the solution for pseudo-steady state for a no-flow outer boundary or continues to use the solution for infinite-acting radial flow. In this model, the changing wellbore storage or dual porosity effects are not considered. The flow equations in pressure are written in the Laplace domain, solved, inverted to real time domain using the Stefhest algorithm (n = 18).

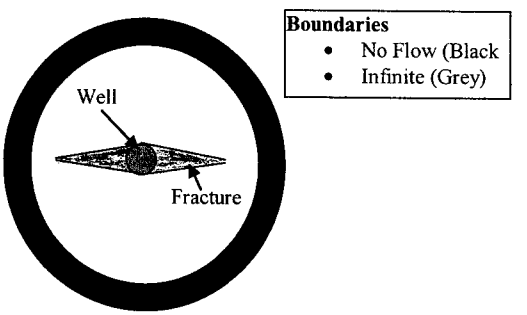

Fig. 1. Finite conductivity fracture model.

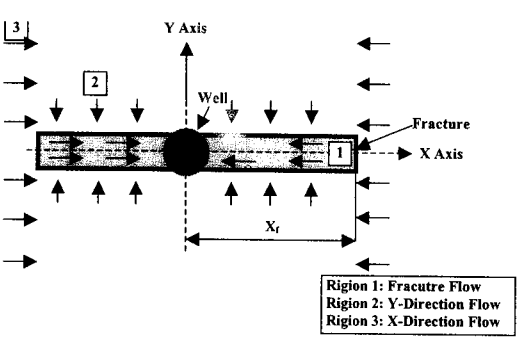

Fig. 2. Tri-linear flow model.

Assumptions

The well intercepts a single fracture in the vertical plane. The finite conductivity fracture model also assumes that there is a pressure gradient along the length of the fracture. The well is at the center of the fracture length. Wellbore storage effect may be present or not.

Bilinear fracture flow behavior

The presence of an artificial fracture modifies the flows near the wellbore considerably. (Cinco-Ley *et al.*, 1985) describes the flows that can be developed around an artificial fractured well. One of them is the bilinear flow.

Bilinear fracture flow occurs in hydraulically fractured wells when the conductivity of the fracture is finite. In this flow regime, two types of linear flow occur in normal direction: one from the matrix to the fracture and one from the fracture to the wellbore. This is usually evident in long fractures (which are hard to prop open effectively) or in natural fractures (which contain fracture fill minerals) (Fig. 3).

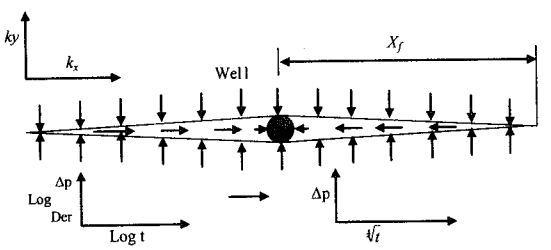

Fig. 3. Schematic diagram of a well completed with a vertical fracture.
(Bilinear fracture flow along the fracture and perpendicular to the fracture).

At early time, after the possible effects of wellbore storage have subsided, the response is bilinear at right angles to the fracture and along the length of the fracture as shown in Fig. 3. On a log-log scale, this is characterized by a quarter unit slope on both the pressure and derivative curves. The quarter unit slope is essentially a very early time feature, and is very often masked by the effects of wellbore storage. After the bilinear flow, the response will become linear flow in the reservoir, characterized by a half-unit slope. When the fracture half-length and formation permeability are known independently, the fracture conductivity $k_f w_f$ can be determined from the bilinear flow regime.

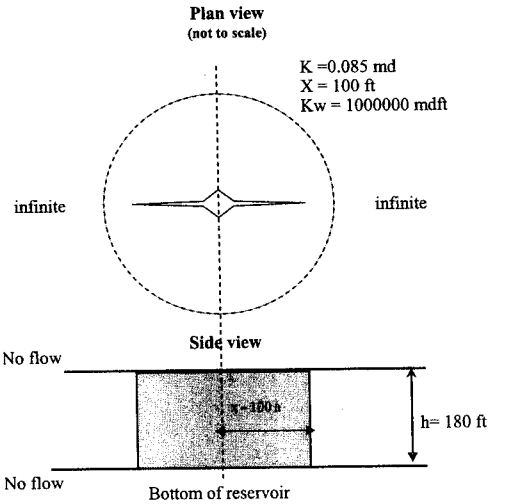

Fig. 4. Schematic sketch of vertical fracture flow.

Non-Darcy flow in vertical fractures

One of the complications that offer special difficulties in interpreting post fracture well performance is non-Darcy flow. (Holditch *et al.*, 1976) studied the effect of non-Darcy flow on the behavior of hydraulically fractured gas wells. They observed in their study that in a build-up test, non-Darcy flow can continue for a substantial time after the well is shut in, and the apparent fracture conductivity can continue to increase throughout much of the test. The non-Darcy flow continues as pressure gradients dissipate during the build-up test because the flow velocity in the narrow fracture remains quite high.

It is normally expected to see non-Darcy flow in gas well tests. This effect will result in creating what we call rate dependent skin. This rate-dependent skin, which is caused by turbulent flow, can be added to any model. The skin for a flow period of rate is given by:

$$Q = S_o + Q * \frac{dS}{dQ} \quad (1)$$

where S_o is the mechanical skin and dS/dQ defines the rate dependence, sometimes called non-Darcy coefficient.

There is also a similar phenomenon, which was seen in these tests, which is non-Darcy flow in the fracture itself. The effect of non-Darcy flow in a hydraulic fracture can be significant causing a large pressure drop in the fracture. This will lead to changing the behavior of the fracture depending on

the velocity of the fluid passing through it. The non-Darcy flow effect is caused by the high velocity of gas in the fracture and will cause the flow to be turbulent and will cause a considerable pressure drop. This makes the fracture appear smaller although it is physically there, and if we reduce the production rate the non-Darcy flow effect will reduce and we may see more of the true characteristics of the fracture. Due to this fact, rate dependent skin was not determined, since it was believed that the non-Darcy flow in fracture represented a bigger portion.

Apparent conductivity

Predicting performance, selecting proppant is based on the non-Darcy effect (Guppy *et al.*, 1982). This showed that effects of non-Darcy flow can be also expressed as an effective or apparent conductivity. They further showed that under certain conditions, non-Darcy effects can be calculated based on two dimensionless parameters:

$$C_{fD} = \frac{k_f w_f}{k\, x_f} \tag{2}$$

The dimensionless fracture conductivity, and for gas wells:

$$Q_D = \frac{k_f\, \rho\, \beta\, q}{w_f\, h\, \mu} \tag{3}$$

Basically the ratio of inertial (i.e., turbulent) drag forces on flow in the fracture to the "Darcy" drag forces.

For gas wells, Eq. (3) (in oil field units) becomes:

$$Q_D = \frac{4.64 \times 10^{-16} k_f\, \beta\, M\, q_g}{w_f\, h\, \mu_{gi}} \tag{4}$$

Several relations were proposed for calculating the apparent conductivity, but the most commonly used relation is:

$$(C_{fD})_{App} = \frac{C_{fD}}{1 + 0.55\, Q_D} \tag{5}$$

This relation is only valid for $C_{fD} < 10$, $Q_D < 2$ (minimal non-Darcy effects, or $C_{fD} > 10$ (for low permeability formations), $Q_D = 1$ to 10. Therefore:

$$(k_f\, w_f)_{App} = \frac{(k_f\, w_f)_{True}}{1 + 0.55\, Q_D} \tag{6}$$

Thus, this relation is effectively limited to low permeability reservoir. This simple relation is received wide expand use as a prognostic tool for the effects of non-Darcy flow.

Bilinear analysis

Bilinear fracture flow is one of the flow regimes that can be identified when a reservoir has a finite conductivity vertical fracture. The purpose of analyzing bilinear flow data is to determine the fracture conductivity, $k_f\, w_f$. Quad Root Time, also known as Bilinear Time $= \sqrt[4]{t}$, is used to analyze data obtained during the bilinear flow regime. Bilinear flow occurs in long fractures with finite conductivity and exhibits a pressure response, which is linear with respect to $\sqrt[4]{t}$. The constant rate solution used to analyze bilinear flow is:

$$\psi_{wf} = \psi_i - 4.43.10^5 \frac{q_g T}{h\sqrt{k_f w_f}} \frac{\sqrt[4]{t}}{\sqrt[4]{k\phi\mu_{gi} c_{ti}}} \tag{7}$$

For a complex sequence of flow rates, the bilinear superposition time function is used. Superposition time is required in order to analyze variable rate, i.e. build-up tests.

Superposition in time involves breaking up a multi-rate sequence into a set of single rates. The rate used for each step is the difference between the current rate and the previous rate. Bilinear flow data will form a straight line when placed on a plot of $\Delta\psi$ vs. $\sqrt[4]{t}$. The slope of this line is used to calculate the root fracture of conductivity, $k_f w_f$ is

$$\sqrt{k_f w_f} = 4.43.10^5 \frac{q_g T}{h.\text{slope}.\sqrt[4]{k\phi\mu_{gi} c_{ti}}} \tag{8}$$

Therefore, the flow period of drawdown and build-up is the $\Delta\psi/q$ vs. $\sqrt[4]{\Delta t_a}$ and ψ vs. $\sqrt{t_c + \Delta t_a} - \sqrt[4]{\Delta t_a}$. The superposition time is also required when multirate analyses are used to approximate situations in which the rate is slowly varying. The formulation of superposition time depends on the flow regime being analyzed. For example, in our case bilinear flow. Therefore, the following formulae are the generalized form of superposition time for bilinear flow regime:

$$t_{\sup,bilinear} = \left[\sum_{j=1}^{N} \frac{(q_j - q_{j-1})}{q_N} \sqrt[4]{(t - t_{j-1})}\right] \quad (9)$$

Equation (9) can handle any number of step changes in rate and for pseudo-steady state, the superposition time function is:

$$t_{sup,pss} = t_c = 24 * \frac{\text{cumulative production}}{\text{flow rate}} \quad (10)$$

Bilinear derivative analysis

Bilinear flow is one of the flow regimes that can be identified at early time when a reservoir has a finite conductivity hydraulic fracture. The signature of bilinear flow data on a derivative plot is a straight line with a slope of 1/4. The position of this line may be used to calculate fracture conductivity, $k_f w_f$, (Eq. (7)). The derivative of this with respect to the natural logarithm o time is:

$$\text{Der} = \frac{1}{4} 4.43.10^5 \frac{q_g T}{h\sqrt{k_f w_f}} \frac{\sqrt[4]{t_a}}{\sqrt{k\phi\mu_{gi}c_{ti}}} \quad (11)$$

This data is then plotted on a log-log plot. Taking the logarithm of the left hand side and the right hand side of the above equations illustrates that a plot of log Der. vs. log t results in a slope of ¼ (the ¼ fraction in front of the log(t) term).

The coordinates of any point on the quarter slope may be used to calculate fracture conductivity.

$$\sqrt{k_f w_f} = \frac{4.43.10^5}{4} \frac{q_g T}{h\sqrt[4]{k\phi\mu_{gi}c_{ti}}} \frac{\sqrt[4]{t_a}}{\text{Der}} \quad (12)$$

Therefore, the root fracture conductivity of drawdown ($\log(\Delta\psi/q)$ vs. $\log(t_a)$) :

$$\sqrt{k_f w_f} = \frac{4.43.10^5}{4} \frac{T}{h\sqrt[4]{k\phi\mu_{gi}c_{ti}}} \frac{\sqrt[4]{t_a}}{\text{Der}} \quad (13)$$

And, for build-up ($\log(\Delta\psi)$ vs. $\log(\Delta t_{eB})$) :

$$\sqrt{k_f w_f} = \frac{4.43.10^5}{4} \frac{q_g T}{h\sqrt[4]{k\phi\mu_{gi}c_{ti}}} \frac{\sqrt[4]{t_c} + \sqrt[4]{\Delta t_a} - \sqrt{t_c + \Delta t_a}}{\text{Der}} \quad (14)$$

Notice that a shift of the quarter slope to the right will correspond to larger fracture conductivity. Bilinear equivalent time, Δt_{eB}, is:

$$\Delta t_{eB} = \sqrt[4]{t_c} + \sqrt[4]{\Delta t} - \sqrt{t_c + \Delta t} \quad (15)$$

The slope of this line is used to calculate the product of the fracture half-length and the square root of permeability:

$$x_f\sqrt{k} = \frac{40.785.10^3\, q_g T}{\text{slope } h\sqrt{\phi\mu_{gi}c_{ti}}} \quad (16)$$

The permeability can be obtained from the radial flow regime analysis or estimated from core data or other tests. Once permeability is determined, fracture half-length can be found.

$$x_f = \frac{x_f\sqrt{k}}{\sqrt{k}} \quad (17)$$

For infinite conductivity fractures, when k_f is large (FcD>20), then the skin factor is:

$$s = \ln\left(\frac{2r_w}{x_f}\right) \quad (18)$$

Pseudosteady state analysis

Pseudosteady state flow is a flow regime that occurs in bounded (closed) reservoirs, after the pressure transient has reached all the boundaries of the reservoir. This includes not only the case of physically bounded reservoirs, but also the case of a well surrounded by other producing wells. In these situations, reservoirs exhibit tank-like behavior. The purpose of analyzing pseudosteady state flow data is to determine the reservoir pore volume, V_p, and original hydrocarbons in place, OOIP or OGIP. This analysis is valid only when the well is flowing. There is no corresponding pseudosteady state analysis for build-up or falloff tests. Pseudosteady state flow cannot be observed in data obtained from build-up or falloff tests. The constant rate solution for analyzing pseudosteady state data is:

$$\psi_{wf} = \psi_i - 1.417.10^6 \frac{q_g T}{kh} * \left[\frac{0.000527k\, t_a}{\phi \mu_{gi} c_{ti} r_e^2} + \ln\left(\frac{r_e}{r_w}\right) - \frac{3}{4} + s' \right] \quad (19)$$

The above equations are linear with time and, as a result, pseudosteady state flow data will form a straight line when plotted on a Cartesian plot.

Productivity index for gas well

Comparison of productivity indices of a well after and before fracture is simple and convenient measure of treatment success. The comparison of productivity indices is more meaningful than the comparison of rates because rate is related to drawdown imposed, and the pressure drawdown in a well before and after fracturing may change dramatically. In contrast, productivity index, the ration of rate to pressure drawdown is influenced more directly by formation and completion properties (Lee *et al.*, 1981; Holditch *et al.*, 1976).

For a gas well, productivity index, PI, is defined as:

$$PI = \frac{q_g}{\bar{\psi}_a - \psi_{a,wf}} = \frac{kh}{141.2\, B_g \mu_g \left[\ln\left(\frac{r_e}{r_w}\right) - \frac{3}{4} + s' \right]} \quad (20)$$

where $\bar{\psi}_a$ is adjusted pressure evaluated at $\bar{\psi}$ (average static drainage area pressure), and $\psi_{a,wf}$ adjusted pressure evaluated at ψ_{wf}, in terms of pressure itself, an adequate approximation to the pseudosteady state flow equation is:

$$\bar{\psi} - \psi_{wf} = \frac{141.2\, q_g B_g \mu_g}{kh} \left[\ln\left(\frac{r_e}{r_w}\right) - \frac{3}{4} + s' \right] \quad (21)$$

where

$$B_g = \frac{10.08 T z}{\bar{\psi} + \psi_{wf}} \quad (22)$$

From the pseudosteady state flow equation for a gas well, the flow equation may be written as:

$$\bar{\psi} - \psi_{wf} = \frac{1,422\, q_g T z \mu_g}{kh} \left[\ln\left(\frac{r_e}{r_w}\right) - \frac{3}{4} + s' \right] \quad (23)$$

$$PI = \frac{q_g \mu_g z}{\bar{\psi} - \psi_{wf}} = \frac{kh}{1,422\, T \left[\ln\left(\frac{r_e}{r_w}\right) - \frac{3}{4} + s' \right]} \quad (24)$$

This equation used to characterize the ability of gas well to produce with a given pressure drawdown.

Pseudo-steady state derivative analysis

The signature of pseudo-steady state data on a derivative plot is a straight line with a unit slope at a late time. The position of this line is used to calculate reservoir pore volume, Vp, and the original hydrocarbons in place, OGIP.

The pseudosteady state flow analysis cannot be applied to data obtained from build-up or falloff tests. The constant rate solution for analyzing PSS flow data is Eq. (19). The derivative of this with respect to the logarithm of time is Eq. (26).

The reservoir pore volume is used to calculate the original hydrocarbons in place:

$$OGIP = G = \frac{V_p (1 - S_{wi})}{B_{gi}} \quad (25)$$

$$Der = \frac{2348\, qT\, t_a}{A h \phi \mu_{gi} c_{ti}} \quad (26)$$

where

$$c_{ti} = c_f + s_{oi} c_o + s_{wi} c_w + s_{gi} c_{gi} \quad (27)$$

This result is linear with time and, as a result, the derivative of PSS data on a log-log plot is a straight line with slope equal to one. Both wellbore storage (early time) and pseudo-steady state (late time) exhibit tank behavior and have a signature of a unit slope on the derivative plot. The coordinates of any point on the late time unit slope may be used to calculate reservoir pore volume (in ft^3).

$$V_p = \phi A h = \frac{2348\, qT}{\mu_{gi} c_{ti}} \frac{t_a}{Der} \quad (28)$$

The reservoir pore volume is used to calculate the original hydrocarbons in place. From the drawdown plot log ($\Delta\psi/q$) vs. log(t_{pssa}) using Eq. (25).

Interpretation methodology of post fracture test (MIT)

Due to non-Darcy flow effects, it was not possible in some cases to match the drawdown and the build-up response simultaneously. Therefore, two models were made; an emphasis was put on matching the final build and drawdown in each test when two models were used. The quality of the match depended on:

- The quality of the rate measurements and,
- The span of the fracture conductivity change due to non-Darcy flow.

Case Studies

The following two field examples are presented to serve and to illustrate the value of looking at this diagnostic model.

Field example 1

The analysis of actual data obtained from the gas well that stimulated by hydraulic fracturing is performed using the model of finite conductivity vertical fracture solution. Table 1 summarized the post frac wellhead and sandface pressure measurements (modified isochronal test). The characteristics of the reservoir as well as the description of the completion are summarized in Table 2.

Table 1. MIT wellhead and sandface pressure measurements

Periods	Duration, hr	Wellhead pressure, psi	Sandface pressure, psi	Flow rate, MMscf/d
Initial shut in		3366	3366	
1st flow 32/64"	12	1347	1750.21	8.207
1st shut in	12	2223	2654.85	
2nd flow 40/46"	12	844	1222.41	8.189
2nd shut in	12	1960	2337.3	
3rd flow 48/64"	12	574	969.9	8.146
3rd shut in	12	1815	2163.38	
4th flow 64/64"	12	335	626.54	8.661
Extend flow 64/64"	48	259	580.6	6.696
Final shut in	110	2564	3058.92	

The modified isochronal post-frac test was analyzed (Fig. 5). This test followed a hydraulic fracture of the well. The fracture was clearly successful, as exhibited by the ½ slope on the derivative plot, and the straight line on the fracture linear flow plot Figs. 6-11 (superposition

Table 2. Reservoir and gas properties (analysis results for Field Example 1)

Finite Conductivity Fracture Gas Well Model (Post-frac test)			
Model Parameters		**Fluid Properties**	
Permeability (k)	0.085 md	Gas Gravity (G)	0.640
Wellbore Storage Constant Dim. (CD)	123.00	CO_2	8.00 %
Fracture Flow Capacity (k_fw)	1000000. md.ft	H_2S	0.00 %
Fracture Face Skin (sf)	0.000	N_2	1.00 %
Fracture Half Length (x_f)	100.000 ft	Critical Pressure (P_c)	703.65 psi
Exterior Radius (r_e)	2978.921 ft	Critical Temperature (T_c)	360.77 R
Turbulence Factor (D)	0.0(MMCF/D)-1	PVT Reference Pressure (P_{PVT})	3400.00 psi
Skin Equivalent to Xf	-5.116	Gas Compressibility (c_g)	2.61514e-4 psi-1
Formation Parameters		Gas Compressibility Factor (z)	0.981
Total Porosity (Φ_t)	3.00 %	Gas Viscosity (μ_g)	0.0193 cp
Gas Saturation (S_g)	70.00 %	Gas Formation Volume Factor (B_g)	0.001079 bbl/scf
Water Saturation (S_w)	30.00 %	**Synthesis Results**	
Oil Saturation (S_o)	0.00 %	Synthetic Initial Pressure (p_i)	3601.57 psi
Wellbore Radius (r_w)	0.30 ft	Flow Efficiency (FE)	1.000
Formation Temperature (T)	285.0 °F	Damage Ratio (DR)	1.000
Formation Compressibility (c_f)	8.014e-6 psi-1	Average Error	1.10 %
Total Compressibility (c_t)	1.922e-4 psi-1	Average Reservoir Pressure	3593.79 psi
Net Pay (h)	180.000 ft	Pressure Drop Due To Fracture Face Skin (#psf)	0.00 psi
Production and Pressure		**Forecasts**	
Final Gas Rate	6.696 MMCF/D	Forecast Flow Duration (t_{flow})	12.00 month
Final Measured Pressure	3052.43 psi	3-Month Constant Rate Forecast @ Curr. Skin	3.741 MMCF/D
Cumulative Gas Production	36.364 MMCF	6-Month Constant Rate Forecast @ Curr. Skin	3.343 MMCF/D
		Constant Rate Forecast @ Curr. Frac. Face Skin	3.020 MMCF/D
		Constant Rate Forecast @ Frac. Face Skin	3.020 MMCF/D
		Forecast Flowing Pressure (P_{flow})	597.98 psi

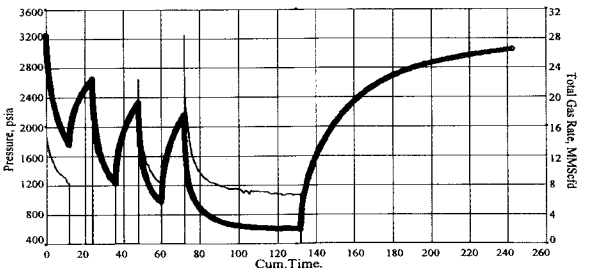

Fig. 5. Post-frac modified isohronal test (bottom hole) - flow rate vs. pressure.

square root time). A fracture half-length of approximately 100 feet is indicated (Fig. 6). The radial flow analysis shows the permeability of the formation to be 0.1md, with a negative skin (due to the frac) of -4.5 (Fig.7).

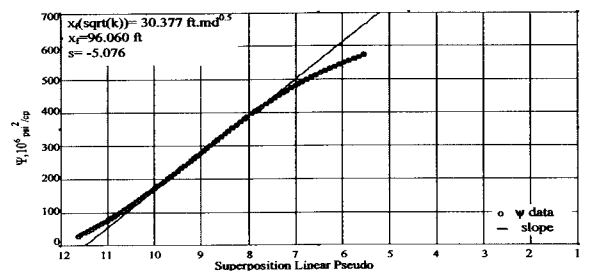

Fig. 6. Fracture linear final build-up.

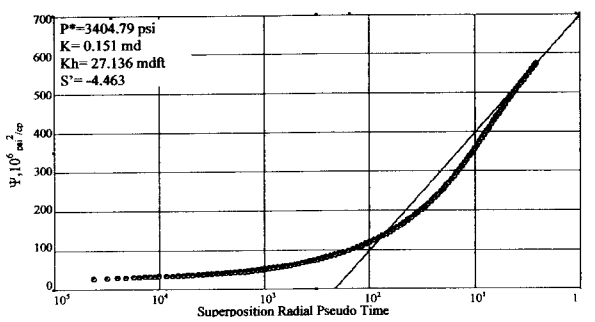

Fig. 7. Final build-up - radial flow extrapolation.

The results of the analyses were used as starting parameters for modeling the test data. The model used was the Finite Conductivity Bounded Reservoir mode (Fig. 4). The results were consistent, and a match of the build-up data was obtained using a frac half-length of 100 ft and a reservoir permeability of 0.085 md (Fig. 8). As expected (in view of the low permeability), reservoir boundaries were not reached during the test period.

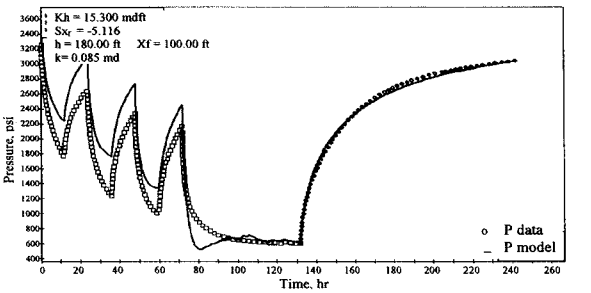

Fig. 8. Finite conductivity fracture (total test overview).

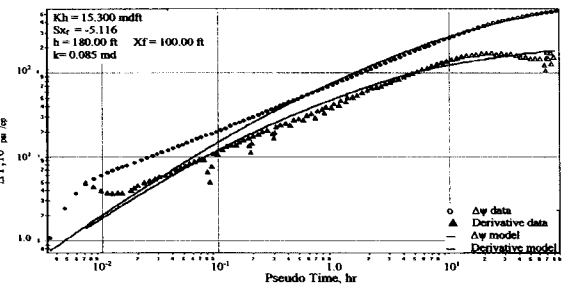

Fig. 9. Fracture model match (finite conductivity fracture type curve).

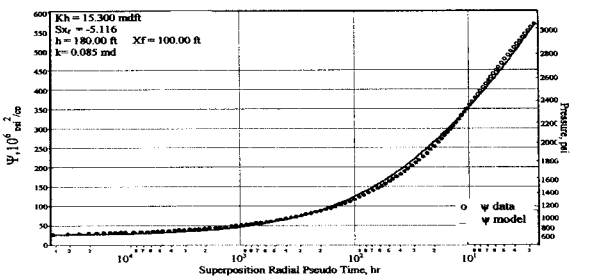

Fig. 10. Finite conductivity fracture model (radial flow analysis).

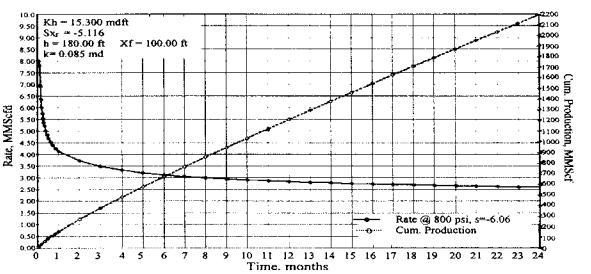

Fig. 11. Finite conductivity fracture transient forecast.

Using the model above, and assuming an infinite size reservoir, a 24-month forecast of production at a flowing sandface pressure of 800 psi was generated. It shows that the deliverability will decline from 7 MMcfd at the time of the test to 3 MMcfd within 12 months (Fig. 11).

The results of the analysis of the modified ischronal post-frac test data confirmed the presence of low permeability (0.1 md) reservoir, skin of -4. The data (wellhead pressures data) were converted to sandface pressures by a multistep calculation that accounts for the variation of gas density with pressure and temperature. The calculated sandface pressures were analyzed by Rate Transient Analysis methods using FAST program.

Field example 2

The effect of the non-Darcy flow during drawdown was high and increased with rate and the fracture characteristics could not be seen as shown on the drawdown derivative plot (Fig. 21). However, during build-up, the bilinear and linear flow periods were seen clearly on all the build-ups as showed in Fig. 14. Therefore, two models were used, one to match the drawdown with its non-Darcy flow effect in the fracture which makes the system looks like a homogeneous system with negative skin, and the other model (fracture with finite conductivity model) was used to match the build-ups.

The analysis and the results of the build-up model are shown in Figs. 12-16, while the analysis and the results, the parameters used of the drawdown model and build-up model are shown in Table 3 and from Figs. 18-22. A summary of the results of the build-up model and the parameters used are shown in Table 3. A history match for the whole test sequence is shown in Fig. 12 and in Fig. 13 for the semi log plot and in Fig. 14 for the main build-up.

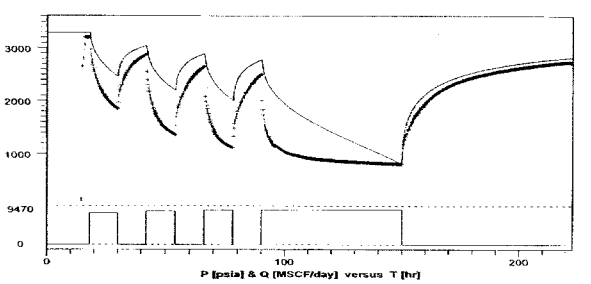

Fig. 12. History match for the whole test sequence.

A history match for the whole test sequence is shown in Fig. 18 and in Fig. 19 for the semi log plot and in Fig. 21 for the main drawdown. The model shows a good match on the drawdown periods.

An attempt was made to calculate the AOFP, but the results showed a reverse trend and therefore do not predict the AOFP. However, the plot is shown

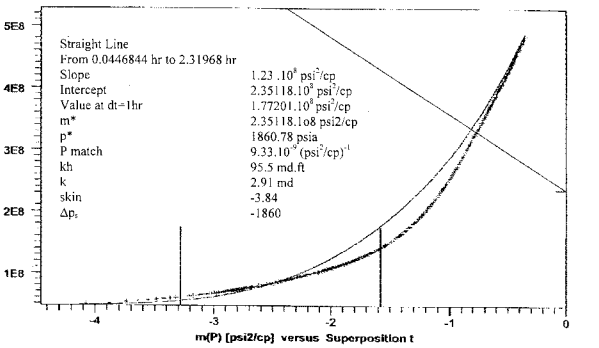

Fig. 13. Semi log plot for the main build-up.

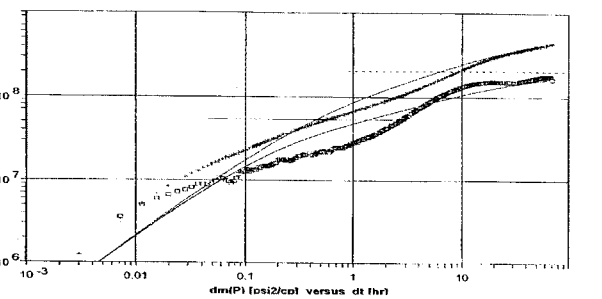

Fig. 14. Pressure build-up data, Log-log plot.

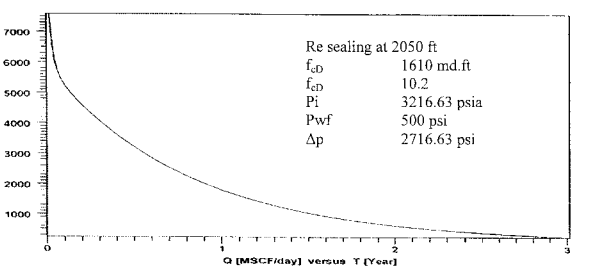

Fig. 15. Rate decline resealing at 2050 ft.

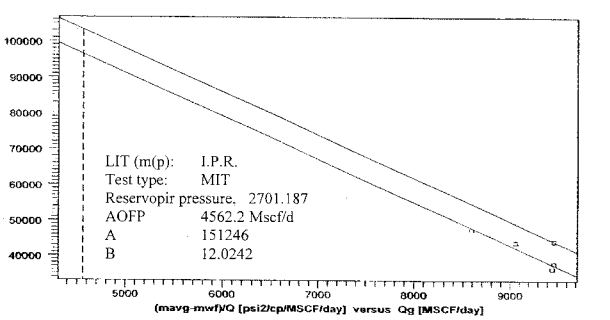

Fig. 16. I.P.R. plot.

Table 3. Detail analysis of build-up and drawdown model cylindrical closed system with a radius of 2050 ft (302.84 acres)

Test Type: Standard	Main Results	
Reservoir and Well Parameters	**Build-up Model**	**Drawdown Model**
Porosity, Φ	6%	6%
Well Radius, r_w	0.354 ft	0.354 ft
Pay Zone, h	32.8 ft	32.8 ft
Flow Period	No.9	No.8
Rate,q	0 Mscf/d	9470 Mscf/d
Rate change	9470 Mscf/d	9470 Mscf/d
P at dt	0 800.21 psi	0 2508.6 psi
Time Match	0.55 hr-1	184 hr-1
Pi	3190 psia	3190 psia
Pressure Match	$2.44*10^{-9}$ (psi/cp)-1	$9.54*10^{-9}$ $(psi^2/cp)^{-1}$
Fluid Type	Gas	Gas
Gas Gravity, γ_g	0.67	0.67
Pseudo Critical P	667.414 psia	667.414 psia
Pseudo Critical T	370.146 R	370.146 R
Reservoir Temperature	300 F	300 F
Reservoir Pressure	3500 psia	3500 psia
Properties at Reservoir T and P		
Total Compressibility, Ct	0.000252405 psi^{-1}	0.000252405 psi^{-1}
Viscosity, μ_g	0.0194304 cp	0.0194304 cp
Reservoir Homogeneous		
Boundary	Infinite	Circle
Well	Frac. Finite Cond	Storage and Skin
Wellbore Storage Coefficient, C	0.69 STB/psi	C 0.00805 STB/psi
Fracture Half Length, X_f	206 ft	
Fracture Conductivity, f_c	1730 md	
Fracture Conductivity Dimensionless, f_{cD}	11.9	
Skin Factor	0	-1.75
Flow Capacity, kh	25 md.ft	97.7 md.ft
Δp_s(skin)		-499.976 psia
Permeability, k	0.76 md	2.98 md
Mobility, k/ μ_g	39.2	153
Investigating Radius, R	396 ft	707 ft
Tested Volume	172846 Barrels	1550096 Barrels

Table 4. Production forecast

	Daily Production in Mscf/d for the Case of 303 Acres at the End of			Daily Production in Mscf/d for the Case of 640 Acres at the End of		
Model	1st Year	2nd Year	3rd Year	1st Year	2nd Year	3rd Year
Drawdown	880	163	9.6	2247	989	461
Buildup	1767	603	233	3104	1926	1207

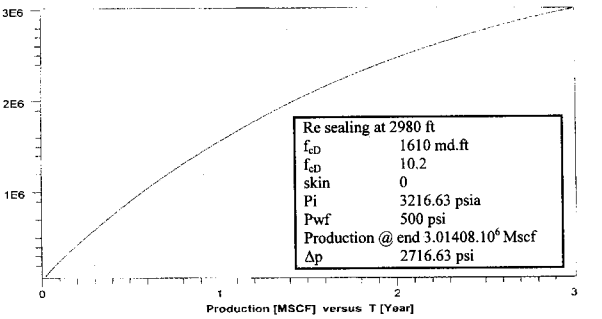

Fig. 17. Build-up data-cumulative production.

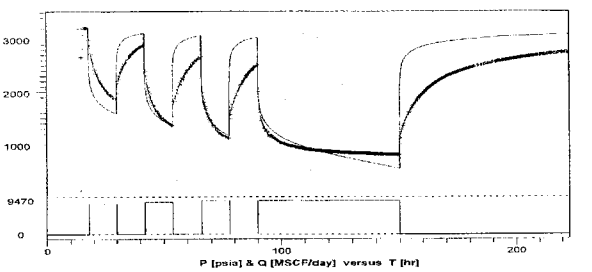

Fig. 18. Drawdown simulation.

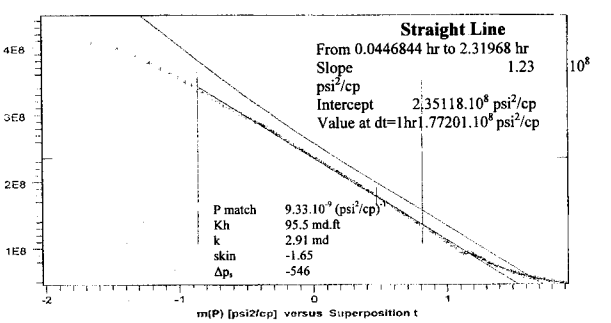

Fig. 19. Drawdown data, semi log.

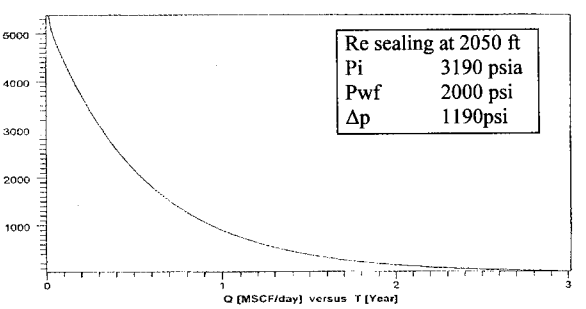

Fig. 20. Rate decline.

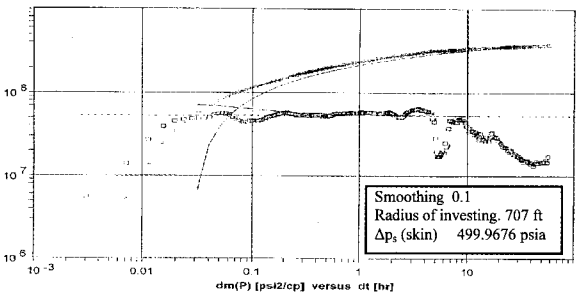

Fig. 21. Drawdown data, log-log plot.

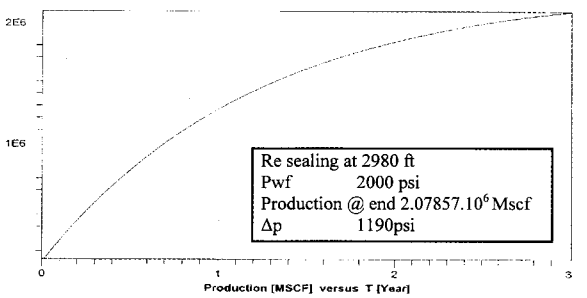

Fig. 22. Drawdown data-cumulative production.

in Fig. 16 for illustration purposes. The plot suggests that with increased drawdown, the rate would decrease. This can be due to two reasons or a combination of them:

- Inaccuracy in rate measurement or lack of stabilization.
- The significant increase in the non-Darcy flow pressure drop with increased rate.

Two scenarios were performed to predict future production using the drawdown and build-up models, with a closed circular boundary with a radius of 2050 ft, which is equivalent to a drainage radius of 303 acres approximately, and are shown in Fig. 15 and Fig. 20. Two more scenarios were also performed using the same models but with a closed circular boundary with a radius of 2890 ft which is equivalent to a drainage radius of 640 acres approximately. The results of the different options are summarized in Table 4.

If the actual drainage area is smaller than that, the rate of decline will be faster. On the other hand, if the formation is fed from a nearby zone, the rate of decline will be reduced. Post-test production data was actually available for this gas well. However, the well was subject to some scale removal operation after the fracture treatment. This scale removal operation is suspected to have caused formation damage to the well. Therefore, the drop in production after this scale removal operation is likely to be caused by this formation damage. It can be also a depletion effect although this is more of a remote possibility.

Conclusions

From the results of this work, the following conclusions are warranted:

- This study implements an improved method for analyzing Modified Isochronal Test in low permeability hydraulically fractured gas wells.
- The effect of non-Darcy flow in fractures is clearly seen in the tests data and will lead to limiting production especially on higher chokes (after one inch). Therefore, non-Darcy effects should be considered in the design of hydraulic fracture treatments, otherwise the design might be far from optimal.
- The non-Darcy flow causes the fracture conductivity to appear lower than its normal value. Therefore, it has predictable effects on the apparent conductivity and on post-frac performance.
- Determination of reservoir permeability and pressure is critical to optimum field development, well completions, and fracture stimulation. Therefore, the modified isochronal test is a viable (practical) means of determining formation permeability.
- The advantages of this study is that it will enable engineers at the operational level to more effectively apply advanced analysis techniques to actual field data, by limiting the possibility of misinterpreting the data.

Nomenclature (Field Units)

A	drainage area, ft^2
AOF	absolute open flow potential, MMcfd
B_{gi}	gas formation volume factor, bbl/scf
$(C_{fD})_{App}$	d. f. c. corrected for non-Dracy
$(C_{fD})_{true}$	true or Laminar D. fracture conductivity
C	wellbore storage, bbl/psi
C_{aD}	apparent wellbore storate constant
C_D	dimensionless wellbore storage constant
c_f	formation compressibility, psi^{-1}
C_{fD}	dimensionless fracture conductivity
c_g	gas compressibility, $psia^{-1}$
C_{pD}	storage pressure parameter
C_t	total system compressibility, psi-1

C_{ws}	compressibility of wellbore fluids, psi^{-1}
Der	derivative
f_c	fracture conductivity, md. ft
FE	flow efficiency
GOR	gas-oil ratio, ft3/bbl
H	fracture height, ft
h	net pay, ft
IPR	inflow performance relationship
$k_{(x,y,z)}$	permeability in the x,y,z direction, md
k_f	fracture permeability, md
$k_f b_f$	fracture conductivity, md.ft
k_{fw}	fracture flow capacity, md. ft
kh	flow capacity, md. ft
P*	extrapolated pressure, psia
p_c	gas pseudo-critical pressure, psia
p_D	dimensionless pressure
PI	productivity index, bbl/d/psi
q	total well flow rate, Mscf/d
Q_D	non-Darcy flow parameter(-)
q_g	gas flow rate, MMcfd/d
q_j	jth flow rate, Msc/d
q_n	nth flow rate, Mscl/d
q_s	stabilized rate – gas, MMcfd/d
r_e	external radius, ft
r_{inv}	radius of investigation, ft
r_w	wellbore radius, ft
s	skin factor
s'	apparent skin factor
s_{gi}	initial gas saturation
S_o	mechanical skin
s_{wi}	initial water saturation
T	temperature, R
T_c	gas pseudo-critical temperature, R
t	shut-in time, hr
$t_{(DA)pss}$	pss dimensionless time at pseudo-steady state
t_a	pseudo-time, hr
tc	effective producing time,hr
t_D	dimensionless time
t_{Dxf}	d. time (based on fracture 1/2 length)
t_n	nth flow period, or superposition time, hr
t_s	time to stabilization, hr
V_p	reservoir pore volume, ft^3
V_{ws}	wellbore volume – gas, ft3
W_f	fracture width, ft
X	intermediate variable
x_f	fracture half-length, ft
Y	intermediate variable
Z	gas compressibility factor
β	non-Darcy flow factor (1/ft)
γ_g	gas specific gravity
Δt	shut-in time, hr
Δt_a	shut-in pseudo time, hr
Δt_e	equivalent time, hr
Δt_{eB}	bilinear equivalent time, hr
μ_i	gas viscosity, cp
ρ_g	gas density, lb_m/ft
Φ	porosity, dimensionless
ψ_i	initial pseudo pressure, psi^2/cp
Ψ_{wf}	flowing pseudo pressure, psi^2/cp
Ψ_{ws}	shut-in pseudo pressure, psi^2/cp

References

Anderson, D. and Mattar, L. "A Systematic and Comprehensive Methodology for Advanced Analysis of Production Data." *SPE*, 8447, (2003).

Barenblatt, G.E. "On Certain Boundary-value Problems for the Equations of Seepage of a Liquid in Fissured Rocks." *J. Appl. Math*, (1963), 460-510.

Barenblatt, G.E.; Zheltov, Iu.P. and Kochina, I.N. "Basic Concepts in the Theory of Homogeneous Liquids in Fissured Rocks." *J. Appl. Math.*, (1960), 1286-1303.

Belani, A.K. and Jalali-Yazdi, Y. "Estimation of Matrix Block Size Distribution in Naturally Fractured Reservoirs." *SPE*, 18171, (Oct. 1988).

Cinco-Ley, H. and Mavor, M.J. "Transient Pressure Behavior of Naturally Fractured Reservoirs." *SPE*, 7977, (Apr. 1979).

Cinco-Ley, H.; Samaniego, F.V. and Kucuk, F. "The Pressure Transient Behavior for Naturally Fractured Reservoirs with Multiple Block Size." *SPE*, 14168, (Sept. 1985), 22-25.

Clark, K.K. "Transient Pressure Testing of Fractured Water Injection Wells." *JPT*, 1821-PA, (June 1968), 639-643.

Crawford, G.E.; Hagedorn, A.R. and Pierce, A.E. "Analysis of Pressure Buildup Tests in Naturally Fractured Reservoirs." *JPT*, 4558-PA, (Nov. 1976), 1295-1300.

DeSwaan, O.A. "Analytic Solution for Determining Naturally Fractured Reservoir Properties by Well Testing." *SPEJ*, 5346-PA, (1976), 117-122.

Fetkovich, M.J. "Decline Curve Analysis Using Type Curves." *JPT*, 4629-PA, (June 1980), 1065-1077.

Gringarten, A.C. and Witherspoom, P.A. "A Method of Analyzing Pumping Test Data from Fractured Aquifer." *Int. Soc. Rock Mech.*, Vol. T3, (1972), T3.

Guppy, K.H.; Cinoco-Ley, H. and Ramey Jr., H.J. "Non-Darcy Flow in Wells with Finite Conductive Vertical Fractures." *SPEJ*, 9291, (1982).

Holditch, S.A. and Morse, R.A. "The Effects of Non-Darcy Flow on the Behavior of Hydraulically Fractured Gas Wells." *SPE*, 6417, *JPT*, (1976).

Horne, R.N. *Modern Well Test Analysis: A Computer Aided Approach.* 2nd ed., Petroway Inc., (1995), 220-225.

Jalali-Yazdi, Y.; Belani, A.K. and Fujiwara, K. "An Interporosity Flow Model for Naturally Fractured Reservoirs." *SPE*, 18749, (Apr. 1989).

Kazemi, H. "Pressure Transient Analysis of Naturally Fractured Reservoirs with Uniform Fracture Distribution." *SPEJ*, 2156-PA, (Dec. 1969), 451–462.

Kazemi, H.; Smeth, M. and Thomas, G.W. "The Interpretation of Interference Tests in Naturally Fractured Reservoirs with Uniform Fracture Distribution." *SPEJ*, 2156-PA, (1969), 463-472.

Kucuk, F. and Sawyer, W.K. "Transient Flow in Naturally Fractured Reservoirs and Its Application to Devonian Gas

Shales." *SPE*, 9397, (Sept. 1980).

Larry, K.; Jack, R.J. and Harmon, H.J. "Application of After-closure Analysis Techniques to Determine Permeability in Tight Formation Gas Reservoir." *SPE*, 90865, (Sept. 2004).

Lee, J. and Brockenbrough, R. "A New Approximate Analytical Solution for Finite Conductivity Vertical Fractures." *SPE*, 12013-PA, (February 1986), 75-88.

Lee, W.J. and Holditch, S.A. "Fracture Evaluation with Pressure Transient Testing in Low-permeability Gas Reservoir." *JPT*, 9975-PA, (Sept. 1981), 1776-1792.

Mattar, L. and Santo, M. "Well Testing of Tight Gas Reservoirs." *SPE*, 100576, (May 2006).

Najurieta, H.L. "A Theory for Pressure Transient Analysis in Naturally Fractured Reservoirs." *JPT*, 6017-PA, (July 1980), 1241–1250

Odeh, A.S. "Unsteady-state Behavior of Naturally Fractured Reservoirs." *SPEJ*, 966-PA, (March 1965), 60-66.

Ohaeri, C.U. "Pressure Buildup Analysis for a Well Produced at a Constant Pressure in a Naturally Fractured Reservoir." *SPE*, 12009, (Oct. 1983).

Partikno, H. "Decline Curve Analysis Using Type Curves-fractured Wells." *SPE*, 84287, (Oct. 2003).

Pollard, P. "Evaluation of Acid Treatment from Pressure Buildup Analysis." Translated, *AIME*, 981-G, (1959), 216.

Prats, M. "Effect of Vertical Fractures on Reservoir Behavior-incompressible Fluid Case." *SPEJ*, 1575-G, (June 1961), 105-118.

Raghavan, R. and Ohaeir, C.U. "Unsteady Flow to a Well Produced at Constant Pressure in a Fractured Reservoir." *SPE*, 9902, (March 1981).

Rahman, A.; Poolad, M. and Mattar, L. "Perforation Inflow Test Analysis (PITA)." *Petroleum Society-Canadian International*, 95510-MS, (June 2005).

Ramey, J. "Non-Darcy Flow and Wellbore Storage Effects in Pressure Buildup and Drawdown of Gas Wells." *JPT*, Vol. 17, (February 1965), 223-223.

Russell, D.G. and Truitt, N.E. "Transient Pressure Behavior in Vertically Fractured Reservoir." *JPT*, 702-PA, (Oct. 1964), 1159-1170.

Streltsova, T.D. "Well Pressure Behavior of a Naturally Fractured Reservoir." *SPEJ*, 10782-PA, (Oct. 1983), 769-780.

Van Everdingen, A.F.V. and Burst, W. "The Application of the Laplace Transformation to Flow Problems in Reservoirs." Translated, *AIME*, 186, (1949), 305-324B.

Warren, J.E. and Root, P.J. "The Behavior of Naturally Fractured Reservoirs." *SPPJ*, 426-PA, (1963), 245-255.

تحليل عملي لاختبار بئر مشقق هيدروليكيًّا في مكمن غازي ذات نفاذية قليلة – دراسة لحالة واقعية

حازم نايل الضمور

قسم هندسة البترول والغاز الطبيعي،

كلية الهندسة، جامعة الملك سعود،

ص ب ٨٠٠، الرياض ١١٤٢١، المملكة العربية السعودية

(قدم للنشر في ٢٠٠٦/١١/٢١م؛ وقبل للنشر في ٢٠٠٧/٠٢/٢٥م)

ملخص البحث. إن الهدف الأساسي من أي عملية تشقيق هيدروليكي للطبقات المنتجة للغاز هو إحداث شقوق متصلة وبطول كافي لتحسين إنتاجية وسلوك آبار الغاز ذات النفاذية القليلة جدًّا، إلا أنه هناك عامل يعتقد أن له أثر سلبي في سلوك هذه الآبار المشققة هيدروليكيًّا والذي يُسمى العامل الذي لا يخضع لقانون دارسي (Non-Darcy flow effect).

يعرض هذا البحث إلى معرفة تأثير هذا العامل والنتائج المستقاة من دراسة تحليل بيانات اختبار (Modified Isochronal Test) بعد عملية التشقق الهيدروليكي لحالة بئر غازي ضمن مكمن للغاز ذو نفاذية قليلة جدًّا ويتقاطع مع شق عامودي عليه، بالإضافة إلى تقدير مواصفات المكمن ومواصفات الشق اللذين اُستخدما في بناء نموذج تحليلي تمت بواسطته عملية استقراء ما يمكن أن تكون عليه إنتاجية البئر بعد التشقق الهيدروليكي.

خلصت الدراسة إلى أن عامل (Non-Darcy flow effect) له تأثير كبير جدًّا على إنتاجية آبار الغاز المشققة هيدروليكيًّا وخصوصًا في حالة انفتاح خانق الإنتاج السطحي على أكبر ما يمكن. لذا يجب الأخذ في الاعتبار تأثير هذا العامل عند عمليات تصميم التشقق الهيدروليكي حتى نحصل على أفضل النتائج المرجوة.

الكلمات المفتاحية: تشقق هيدروليكي، مكمن غازي ذو نفاذية قليلة، سلوك بئر الغاز، العامل الذي لا يخضع لقانون دارسي، تأثير الشق ذو النفاذية المحدودة، اختبار الآبار MIT.